Near-Field Short Range Correlation in Optical Waves Transmitted through Random Media

V. Emiliani,* F. Intonti, M. Cazayous,† D. S. Wiersma, and M. Colocci
National Institute for the Physics of Matter and European Laboratory for Nonlinear Spectroscopy, Via Nello Carrara 1, 50019 Firenze, Italy

F. Aliev
University of Puerto Rico, San Juan, Puerto Rico 00931, USA

A. Lagendijk
Department of Applied Physics and MESA+ Research Institute, University of Twente, 7500 AE Enschede, The Netherlands
(Received 14 November 2002; published 24 June 2003)

Two-dimensional near-field images of light transmitted through a disordered dielectric structure have been measured for two probe wavelengths. From these data, the 2D spatial dependence of the intensity correlation function, $C(\Delta\vec{R})$, has been extracted. We observe that the spatial dependence of C is dominated by a rapidly varying feature determined by the wavelength of the probe light and the average refractive index of the material, as expected by theory. Finally, we deduce the absolute value of the effective refractive index by fitting the theoretical spatial dependence of C to our experimental results.

DOI: 10.1103/PhysRevLett.90.250801 PACS numbers: 07.79.Fc, 42.25.Dd, 42.30.–d, 78.35.+c

During the past decades, the field of light waves propagation in disordered dielectrics has attracted considerable interest due to its fundamental importance, and in view of its potential application in photonics, medical, and biological research. From the fundamental point of view, random multiple scattering of light waves shows many similarities with the propagation of electrons in metals, and various electron transport phenomena have now also be found to exist for light waves in disordered dielectrics. Important examples are the photonic Hall effect [1], universal conductance fluctuations [2], coherent backscattering or weak localization of light [3,4], and Anderson localization [5]. In the optical frequency range, the basic understanding of light diffusion is important in view of its application in medical diagnostic. Near-infrared diffuse light is nowadays largely used to view body function and structures [6–8]. This is made possible by a spectral window that exists within tissue in the 700–900 nm region, in which photon transmission is dominated by diffusive scattering. Moreover, diffusing wave spectroscopy [9,10] is extensively used for the investigation of the structural and dynamic properties of materials that strongly scatters light, colloidal suspensions [11], complex fluids [12], and motor proteins [13].

In disordered dielectric structures, electromagnetic waves are randomly scattered through complicated multiple scattering processes [14]. As a result, the spatial distribution of the transmitted waves shows the typical complicated granular pattern also referred to as bulk speckle. The existence of this speckle pattern is a demonstration of the fact that interference effects survive the random multiple scattering process. A speckle pattern contains vast information about the particular realization which produced it and can be described in statistical terms. The statistical properties are well represented by the correlation function, $C = \langle \delta I \delta I' \rangle$, where $\delta I = I - \langle I \rangle$ is the spatial or temporal fluctuation of the intensity with respect to its average value. The correlation function C contains three terms describing short range (C_1), long range (C_2), and infinite range (C_3) correlations [15–18].

In the weak scattering limit ($k\ell \gg 1$, where $k = 2n\pi/\lambda$ and ℓ is the light mean-free path, n the refractive index of the material), the main contribution to C is the *short range* correlation term which is given by the square of the field correlation function: $C_1 = |\langle EE'^* \rangle|^2$. The spatial dependence of C_1 for a monochromatic source has been calculated by Shapiro [15] and is given by $(\sin k\Delta r/k\Delta r)^2 \exp(-\Delta r/\ell)$. This expression shows that the correlation in a speckle pattern decreases exponentially with the mean-free path, modulated by the feature $(\sin k\Delta r/k\Delta r)^2$ oscillating on the scale of the wavelength. By defining a correlation length δr as the first zero of the fine structure, the short range correlation term tells us that in the weak scattering regime there will always exist a lower limit to the correlation length, given by the probe wavelength.

While the far-field properties, such as the memory effect [19] or coherent backscattering, have been demonstrated for optical waves [3,4], the spatial oscillations in the short range correlation, which are intrinsic properties of the near-field intensity distribution, have been so far observed only for microwave radiation [20].

In this paper, we report on the two-dimensional (2D) short range correlation of the intensity distribution of the transmitted light waves that have been multiply scattered through a disordered medium. By using an aperture scanning near-field optical microscope (SNOM), we collect images of the intensity patterns for different probe wavelengths. The autocorrelation of these images shows the 2D subwavelength modulation as predicted by theory.

The dependence of the observed modulations on the refractive index of the sample is verified by reversibly modifying the value of n by infiltrating the sample with water. Finally, by fitting the theoretical spatial dependence of C_1 to our data, we can deduce the effective refractive index of the sample.

The sample under study is a disordered dielectric structure of microporous silica glass with randomly oriented and interconnected pores $\simeq 200$ nm in size. The thickness of the sample is $\simeq 1.7$ mm; the surface area is $\simeq 4 \times 6$ mm^2.

Spatially resolved near-field images of the speckle patterns are collected with a commercial (Twinsnom, OMICRON) scanning near-field optical microscope used in the illumination mode. Light from a He-Ne (632 nm) and a diode laser (780 nm) is transmitted through a commercial (Nanonics) pulled coated near-field probe with a nominal aperture $L \leq 100$ nm. The spot of the diffusely transmitted light through the sample is imaged onto the entrance of a GaAs photomultiplier. The solid angle of collection is 0.36 sr.

Near-field optical maps are recorded by scanning the sample with respect to the near-field probe and by acquiring, for each probe position, the corresponding integrated intensity of the diffusely transmitted light. The wavelength dependence is obtained by coupling simultaneously the different lasers into the optical fiber. Selection of the probe wavelength is done via the laser shutters. The transport mean-free path of photons in the sample is derived from the diffusion constant as measured in a time resolved transmission experiment, following the configuration of Ref. [21].

Figure 1 shows a 10×10 μm^2 shear force image of the sample surface. A cross section through the image (not shown) reveals a mean size of the pores in the range of 100–200 nm and a volume fraction of pores of about 30%. Using the geometrical average, we can estimate the average refractive index to be $n_{av} = 1.3$. The geometrical average refractive index is expected to be about 10% to 20% higher than the actual effective refractive index [22].

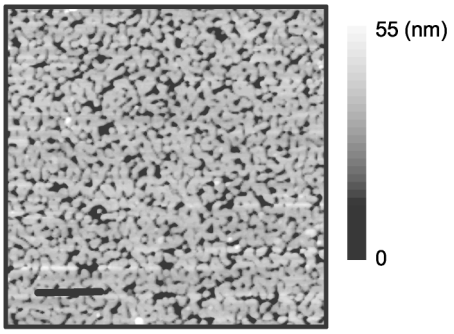

FIG. 1. 10×10 μm^2 shear force image of the sample surface. A cross section through the image (not shown) reveals an average size of the pores of 150 nm and a volume fraction of roughly 30%. Bar $= 2$ μm.

Figures 2(a) and 2(b) show two-dimensional maps of the transmitted intensity, $I(\vec{R})$, as a function of the near-field probe position for two different excitation wavelengths: 780 and 632 nm. In both images, intensity maxima and minima are visible on top of a quasiuniform background. The last is due to the finite spatial resolution (150 nm) of our apparatus and possibly to a far-field component in the collected data. The optical contrast is between 40% and 50%.

Interesting information about the light distribution can be deduced once the 2D intensity correlation functions, $C(\Delta\vec{R}) = \langle \delta I(\vec{R}) \delta I(\vec{R} - \Delta\vec{R}) \rangle$, are calculated. The results for 632 and 780 nm incident wavelengths are shown in Figs. 3(a) and 3(b), respectively. The images show a peak in the center, which corresponds to $\Delta\vec{R} = 0$. Radially from the center, a series of maxima and minima indicate the subwavelength oscillatory components of the correlation function. As can be noted in the figure, the spatial distribution scales with the excitation wavelength. It is also evident that the images show a symmetry axis which is not expected by the theory. We believe that the observed axis of symmetry is a result of the tip shape. As a matter of fact, it has different orientations for different tips. On the contrary, it maintains the same orientation when we keep the same tip while varying the incident wavelength. The experimental asymmetry can be reproduced by the convolution of an elliptic aperture on the tip with the theoretical intensity pattern. Measurements are in progress to better address this point.

The oscillatory behavior of $C(\Delta\vec{R})$ shown in Fig. 3 is even more apparent by looking at the radial sections plotted in Figs. 4(a) and 4(b), where $C(\Delta R)$, with $\Delta R = |\Delta\vec{R}|$, is plotted for the two different excitation wavelengths [insets: $C(\Delta R)$ reported in a logarithmic scale]. Apart from the pronounced maximum centered at $\Delta R = 0$ ($\simeq 200$ nm in width), a first minimum at 300 and 275 nm is found for $\lambda = 780$ and 632 nm, respectively, followed by three successive maxima with a rapidly decaying intensity.

In order to stress the dependence of $C(\Delta\vec{R})$ on the refractive index of the material, we have increased the value of n by infiltrating the sample with few drops of water. Because of the predicted (see below) dependence of C on λ/n, this change should induce a shift in the correlation curves to shorter distances.

Two-dimensional images of transmitted light were acquired on the same scan region, before (empty dots) and after (full dots) the infiltration of the sample. The probe wavelength was 780 nm. Cross sections through the corresponding 2D correlation function C are compared in Fig. 5. The peak positions in the curve for the infiltrated sample move, as expected, to shorter values of ΔR.

The dependence of our data on the probe wavelength and on the refractive index represents a good proof of the

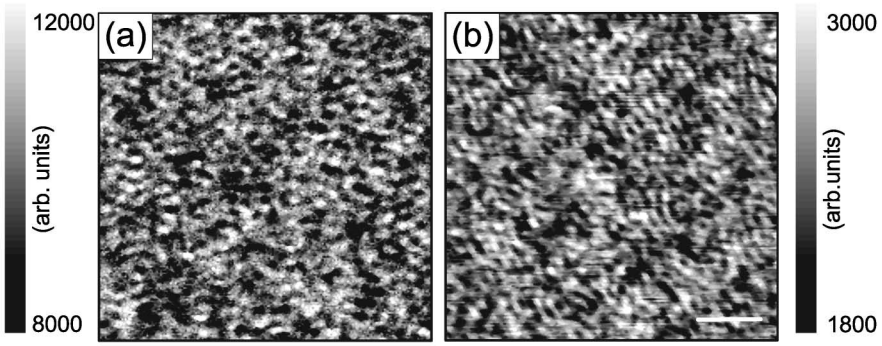

FIG. 2. Two-dimensional near-field optical image of the integrated intensity of the transmitted light as a function of the tip position for two probe wavelengths: (a) 780 nm and (b) 632 nm; Bar = 2 μm.

absence of topographic artifacts. This point has been further addressed by calculating 2D correlation functions of the shear force signal. Radial sections through those images (not shown) present a central peak about 200 nm in size and, contrary to the optical correlations, they do not show extra features.

The normalized spatial intensity correlation function is defined as

$$C(\Delta r, \Delta R) = \langle \delta I(\vec{r}, \vec{R}) \delta I'(\vec{r}', \vec{R}') \rangle / \langle I(\vec{r}, \vec{R}) \rangle \langle I(\vec{r}', \vec{R}') \rangle, \tag{1}$$

where $\delta I = I - \langle I \rangle$ is the spatial deviation of the intensity from its ensemble average value, $\Delta r = | \vec{r} - \vec{r}' |$ and $\Delta R = | \vec{R} - \vec{R}' |$ are the radial displacements across the output and input surfaces, respectively, and the brackets $\langle \cdots \rangle$ represent the ensemble average.

The normalized intensity correlation function can be written as the sum of three terms: C_1, C_2, and C_3, describing short, long, and infinitive range correlations, respectively. The dominating contribution to C in our system is most likely given by the short range correlation term C_1.

It has been shown [20] that $C_1(\Delta r, 0)$ and $C_1(0, \Delta R)$ are equivalent as required by reciprocity [23]. In our experimental configuration, the sample is moved with respect to the source and the transmitted light is collected by a fixed detector with a solid angle of collection of 0.36 sr. The total number of independent speckle spots in transmission is given by $N = 2\pi W/\lambda^2$ [17,24], with W the radiating area of the output surface of the sample. At our solid angle of collection, we collect a fraction of 0.057 of these independent speckle spots. This gives a number of collected speckle spots, N_c, $\simeq 1.3 \times 10^6$ at 780 nm and $\simeq 2.0 \times 10^6$ at 632 nm. Hence, our correlation function is normalized by a factor $A = 1/\sqrt{N_c}$, with N_c as given above. This means that we actually measure the function $AC_1(0, \Delta R) = A \times F(\Delta R)$.

For the case of a point source in an elastic scattering medium, the function $F(\Delta R)$ has been calculated by factorizing the fields [15]:

$$F(\Delta R) = | \langle E(\vec{r}, \vec{R}) E^*(\vec{r}', \vec{R}') \rangle |^2 / \langle I(\vec{r}, \vec{R}) \rangle \langle I(\vec{r}', \vec{R}') \rangle$$

$$= \left(\frac{\sin(k\Delta R)}{k\Delta R} \right)^2 \exp(-\Delta R/\ell). \tag{2}$$

Equation (2) predicts that the short range correlation term is dominated by a rapidly varying structure determined

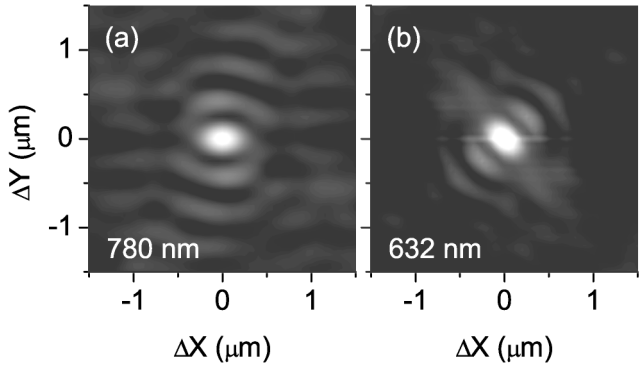

FIG. 3. Two-dimensional spatial dependence of the intensity correlation function $C(\Delta \vec{R})$ for (a) 780 nm and (b) 632 nm probe wavelengths.

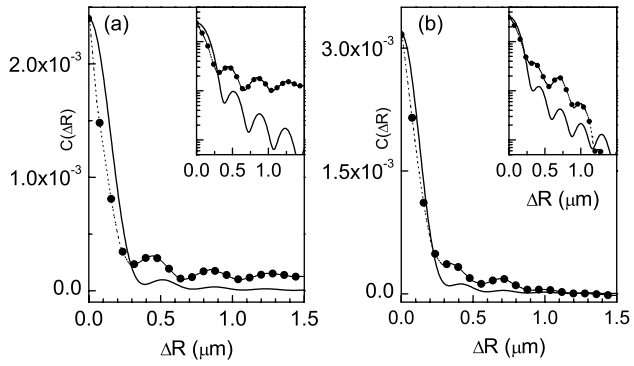

FIG. 4. Averaged radial profile (dots) through (a) Fig. 3(a), probe wavelength of 780 nm, and (b) Fig. 3(b), probe wavelength of 632 nm. The corresponding theoretical fits are shown in solid lines; to account for the finite size aperture, L, the theoretical curves are convoluted with a Gaussian of width $\sigma = \sqrt{2} \times L$. Insets: Same functions reported in logarithmic scale. The dashed lines are a guide for the eye.

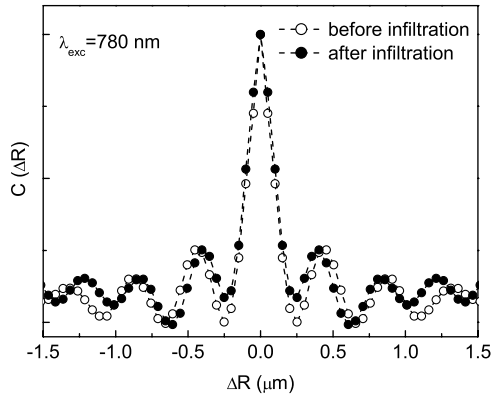

FIG. 5. $C(\Delta R)$ measured for a probe wavelength of 780 nm, before (empty dots) and after (full dots) infiltration with water. The two curves are normalized to one. The dashed lines are a guide for the eye.

by the wavelength of the incident light and the refractive index of the material.

For the sample under investigation, the measured ℓ is about 10 μm. Therefore the exponential term can be neglected since the spatial region where the oscillations are experimentally observed (2 μm) is much shorter than ℓ. The radial section through the images of Fig. 2 is fitted by the following expression: $AC_1(\Delta R) = A \times (\frac{\sin(k\Delta R)}{k\Delta R})^2$, where A is expected to be of the order of $1/\sqrt{N_c}$, and the scaling factor A and the effective refractive index n are the only fitting parameters. The fitted curves, Gaussian-convoluted in order to account for the finite tip aperture, are reported in Figs. 4(a) and 4(b). We found good agreement between theory and experimental data by taking for n a value of $n = 1.1 \pm 0.1$.

As previously discussed, the optical contrast in the images reported in Figs. 2(a) and 2(b) is approximately 50%. We believe that this is the main effect that masks the zeros of the correlation function by adding an offset to the curve.

In conclusion, near-field optical images of the speckle patterns formed by optical waves transmitted through a random medium have been measured. From the two-dimensional images, a map of the intensity correlation function has been obtained. The predicted existence of short range correlation in the transmitted pattern and its dependence on the incident wavelength and on the refractive index was verified. By fitting the theory to our data, the effective refractive index of the medium is extracted. The good agreement between experimental results and theoretical prediction provides the first experimental evidence of the two-dimensional spatial distribution of C_1 for optical waves.

We thank Massimo Gurioli, Patrick Sebbah, and Azriel Genack for helpful discussions. This work was supported by the European Community under Contract No. HPRICT1999-00111 and by the INFM project PHOTONIC. F. A. acknowledges the American Chemical Society Petroleum Research Fund for partial support of this research.

*Electronic address: emiliani@lens.unifi.it
†Permanent address: Laboratoire de Physique des Solides, University Paul Sabatier, 31062 Toulouse, France.

[1] B. A. van Tiggelen, Phys. Rev. Lett. **75**, 422 (1995).
[2] F. Scheffold and G. Maret, Phys. Rev. Lett. **81**, 5800 (1998).
[3] M. P. Van Albada and A. Lagendijk, Phys. Rev. Lett. **55**, 2692 (1985).
[4] P.-E. Wolf and G. Maret, Phys. Rev. Lett. **55**, 2696 (1985).
[5] S. John, Phys. Rev. Lett. **53**, 2169 (1984); P.W. Anderson, Philos. Mag. B **52**, 505 (1985).
[6] A. Yodh and B. Chance, Phys. Today **48**, No. 3, 34 (1995).
[7] A. Dubois, L. Vabre, A. C. Boccara, and E. Beaurepaire, Appl. Opt. **41**, 805 (2002).
[8] M. Xu, M. Lax, and R. R. Alfano, J. Opt. Soc. Am. A **18**, 1535 (2001).
[9] G. Maret and P. E. Wolf, Z. Phys. B **65**, 409 (1987).
[10] D. J. Pine, D. A. Weitz, P. M. Chaikin, and E. Herbolzheimer, Phys. Rev. Lett. **60**, 1134 (1988).
[11] S. Romer, F. Scheffold, and P. Schurtenberger, Phys. Rev. Lett. **85**, 4980 (2000).
[12] T. G. Mason and D. A. Weitz, Phys. Rev. Lett. **74**, 1250 (2002).
[13] L. LeGoff, F. Amblard, and E. M. Furst, Phys. Rev. Lett. **88**, 018101 (1995).
[14] See, for instance, Ping Sheng, *Introduction to Wave Scattering, Localization, and Mesoscopic Phenomena* (Academic, New York, 1995).
[15] B. Shapiro, Phys. Rev. Lett. **57**, 2168 (1986).
[16] M. J. Stephen and G. Cwilich, Phys. Rev. Lett. **59**, 285 (1987).
[17] S. Feng, C. Kane, P. A. Lee, and A. D. Stone, Phys. Rev. Lett. **61**, 834 (1988).
[18] A. Z. Genack, N. Garcia, and W. Polkosnik, Phys. Rev. Lett. **65**, 2129 (1990).
[19] I. Freund, M. Rosenbluh, and S. Feng, Phys. Rev. Lett. **61**, 2328 (1988).
[20] P. Sebbah, B. Hu, A. Z. Genack, R. Pnini, and B. Shapiro, Phys. Rev. Lett. **88**, 123901 (2002).
[21] D. S. Wiersma, M. Colocci, R. Righini, and F. Aliev, Phys. Rev. B **64**, 144208 (2001).
[22] P. N. den Outer and A. Lagendijk, Opt. Commun. **103**, 169 (1993).
[23] R. Carminati, J. J. Saenz, J. J. Greffet, and M. Nieto-Vesperinas, Phys. Rev. A **62**, 12712 (2000).
[24] M. P. van Albada, J. F. de Boer, and A. Lagendijk, Phys. Rev. Lett. **64**, 2787 (1990).